Anti-short-circuit device: a new solution for short-circuiting in windcatcher and improvement of natural ventilation performance

Payam Nejat[1], John Kaiser Calautit[2*], Muhd Zaimi Abd. Majid[3], Ben Richard Hughes[2], Fatemeh Jomehzadeh[1, 4]

1: Faculty of Civil Engineering, Universiti Teknologi Malaysia, UTM- Skudai, Johor, Malaysia

Email: payam.nejaat@gmail.com

2: Department of Mechanical Engineering, University of Sheffield, Sheffield, UK

Email: J.Calautit@sheffield.ac.uk , Tel: +44 (0) 7544158981

3: Construction Research Center, Institute of Smart Infrastructure and Innovative Construction, Universiti Teknologi Malaysia, Johor, Malaysia

4: Advanced Built and Environment Research (ABER) center, Tehran, Iran

Abstract

Windcatcher is an effective technique for naturally ventilating a space and improving indoor air quality. A common problem for modern and traditional windcatchers is air short-circuiting. Air-short-circuiting in windcatchers occurs when the air entering through the supply channel immediately exits through the exhaust channel without circulating and mixing inside the enclosed space. Several previous works on windcatchers have observed the "short-circuiting" effect and concluded that it has a negative impact on the ventilation performance however, no work have provided a solution to eliminate this effect. The present study will address this issue by incorporating a component called the anti-short-circuiting device (ASCD) and investigating its potential to eliminate air short-circuiting in windcatchers and improve ventilation performance. Two methods were employed in this research: experimental and Computational Fluid Dynamics (CFD) study. For the experimental work, three scaled models were studied in a wind tunnel. The CFD modelling was validated using the air velocity measurements and good correlation was observed with average error below 10%. The results showed that the ASCD windcatcher with angles between 20°-80° prevented air-short-circuiting while supplying up to 40-51 l/s per occupant, which is higher than the minimum recommendations of ASHRAE62.2 and BS5925. In addition, the windcatcher without ASCD showed 8% higher CO_2 concentration in the room, indicating that the ASCD windcatcher was more effective in removing stale air out of the room. Furthermore, the average air velocity in the room at sitting height with the ASCD windcatcher was 19-28% higher than windcatcher without ASCD.

Keywords: Windcatcher; Natural ventilation; Short circuit; Indoor air quality; Fin; Badgir

1. Introduction

Buildings are responsible for 40% of the global energy consumption and accounts for around 30% of the carbon emissions all over the world [1]. Moreover, almost 60% of total energy consumption in buildings is used for Heating, Ventilating, and Air conditioning (HVAC) systems [2]. Generally, it is required that the HVAC system energy use is minimized but without compromising the comfort and health of occupants [3]. Since people spend 80% to 90% of their time in indoor spaces, appropriate indoor air quality (IAQ) and comfort must be provided [4]. One promising solution that has gained attention is the incorporation of natural ventilation in buildings [5]. Recently, natural ventilation techniques such as windcatchers are increasingly being employed in buildings for increasing the fresh air rates and reducing the energy consumption [6].

A windcatcher can be defined as an architectural element placed on the building roof [7], which provides fresh air to the interior living spaces and release stale air through windows or other exhaust segments [8]. It is not straightforward to ascertain the first origin of windcatcher in the world. However, during archaeological investigations conducted by Masouda in 1970s, the first historical evidence of windcatcher was found in the site of Tappeh Chackmaq near Shahrood, Iran which dates back to 4000 BC [9,10]. Traditionally, windcatcher has been utilized in Persian Gulf countries such as Iran, Iraq, Qatar and Emirates as well as North Africa region like Egypt and Algeria [11].

Bahadori et al. [12] stated that the main benefit of windcatcher, like other passive technologies, is that it exploits wind renewable energy for their operation so they are considerably cost effective and more healthier. In addition to improving human comfort, they have low maintenance cost due to having no moving parts, capturing and supplying clean and fresh air at roof level compared to low level windows [13]. Although it has many advantages, a problem of both modern and traditional multi-channel windcatchers is air-short-circuiting that is reported by different scholars in previous studies [14–19] and has a negative impact on the ventilation performance of windcatcher. Air-short-circuiting occurs when the air entering through the supply channel immediately exits through the exhaust without circulating inside the enclosed space (see

Fig. 1) [8,20]. Montazeri claimed that short-circuiting is one of the most influencing factor in decreasing the efficiency of a multi-channel windcatcher system [8].

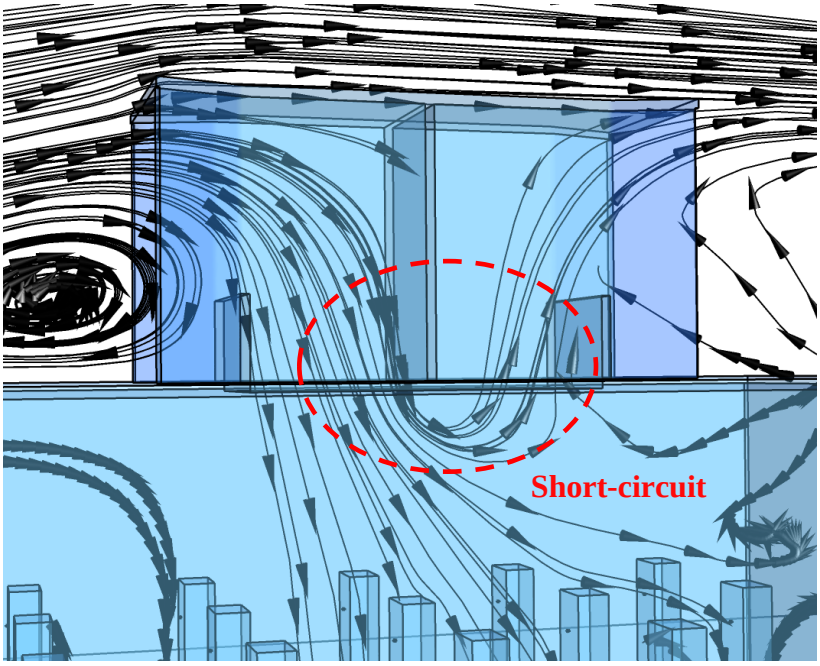

Fig. 1. Air-short-circuiting in a room with a two-sided windcatcher.

Montazeri et al. [15] studied a reduced-scale model (1:40) of two-sided windcatcher for various air incident angles in a wind tunnel. Moreover, the work developed numerical CFD and analytical models to validate the accuracy of the experimental results. It was established that for high air incident angles, short-circuiting appears into the wind tower system and reaches its maximum value at air incident angle of 60.

Hughes & Ghani [16] carried out the CFD modelling of a four-sided windcatcher to analyze the effect of the control mechanism of air flow inside the system. In the CFD study, nineteen numerical models were created in different damper angles range of 0–90° with an interval of 5°. The computational results indicated that the optimum operating occurs at a damper angle range of 45 to 55° which in this angle the minimum of short-circuit was observed compared with other angle.

Hughes and Ghani [21] conducted a CFD study of a commercial windcatcher ventilation performance and compared against current British Standards. The different wind direction was

simulated in order to find the effect of the dampers on the flow, and whether they can reduce some of the short-circuiting phenomena. The results showed that when the flow is counter current to the direction of the damper a higher velocity was observed through the diffuser, which specifies that some of the short-circuiting has been removed by the damper and averagely, the delivered performance was improved by nearly 5%.

Afshin et al. [22] also investigated the natural ventilation performance of a two-sided windcatcher for various wind angles using wind tunnel and smoke testing. The smoke testing revealed that the air streams towards the bottom of the windcatcher channel are divided into two; the first stream tends to move to the room below. The second stream tends to move to the leeward side of the windcatcher and leaves the exhaust opening without flowing inside the room (short-circuiting).

From the review of the literature, it can be summarized that a few of studies concluded that the air-short-circuiting is a major inefficiency factor. Although some of researchers paid attention toward the role of damper to reduce this problem, none of them offered a solution to eliminate it. Hence, due to the lack of knowledge in this field, this research takes an opportunity to improve the ventilation performance of windcatcher by employment a new component which is called in this paper as anti-short-circuit device (ASCD) to direct the air flow as a fin. Therefore, the objectives of current research are the following:

- First, to study the effect of ASCD on the short-circuit problem and compare the performance of the windcatcher with ASCD and the reference windcatcher (without ASCD) in low wind speed climate of Malaysia.
- The second objective is to determine the influence of ASCD on indoor air quality and CO_2 concentration inside the building and also the exhaust airflow.

It should be noted that, although damper and ASCD have some similarities, the main function of damper is to reduce air flow rate and prevent from high air velocity entering the interior space, however, the function of ASCD is to direct and guide the air flow to prevent from short-circuit and make more efficient air circulation. Hence, damper is utilized in area with high wind speeds

such as the UK [21] and cannot have functionality in low wind speed climate but ASCD can be used in low wind speed climate (such as Malaysia) to improve the ventilation performance.

2. Research methodology

This research employed two investigative methods: experimental and computational fluid dynamics (CFD) study. Previous studies proved that these methods are reliable in terms of evaluating the ventilation performance of windcatchers [23] . The experiment can be done in either full-scale or reduced-scale wind tunnel test. Like many previous works that assessed the windcatcher, the wind tunnel test was selected for the experimental study because a controllable environment was necessary to study the effect of different flow speeds and also due to the lower cost. In addition, the reduced-scale model can predict the behavior of the flow same as the full scale model provided that the similarity in geometry and Reynolds number are achieved [24]. Both of these research methods are explained in the following sections in details.

2.1 Experimental procedure and wind tunnel set-up

In aerodynamic research, the Reynolds number determines the patterns of air flow around a building and the related wind loads. Thus, the reduced-scale model tested in wind tunnel should ideally experience the same Reynolds number exactly as the actual case in a real environment [6,15,24]. Nevertheless, even in very large wind tunnels which can run at high wind speeds, it is usually difficult to simulate scaled models at exactly similar Reynolds number as it will be in a full scale environment. But, if the Reynolds number is not less than 10,000, the similarity of Reynolds number for the model and real object for sharp edges of model is negligible because flow separation occurs fixedly in these sharp points regardless of Reynolds number and thus, the wind reaction is nearly independent from Reynolds number [6]. In this study it was ensured that Reynolds number value was above the acceptable range by running the wind tunnel at 10 m/s.

One of the potential challenging issues of wind tunnel testing is blockage which can be defined as model frontal area over test section cross-sectional area. It is suggested to select suitable scaling factor that can achieve blockage of less than 5% [25]. Models with relative dimensions larger than this would force the air flow to be squeezed between the model and wind tunnel walls in an unrealistic manner which require blockage corrections [6,8] and [25]. Therefore, to avoid

the above matter with considering test section area and model cross-sectional area, the model was scaled down by 1:10 to achieve a blockage less than 5%.

Generally, windcatchers are classified in five groups of one-sided, two-sided, four, six and eight-sided. Based on the study [8], the efficiency of the two-sided is higher than other types, particularly in zero wind incident angle, which can induce the most volume of air flow into the room. Hence, this type is a typical conventional windcatcher in regions with predominant wind direction [15] and [26]. Therefore, two-sided windcatcher was selected for this study due to predominant wind direction (northeast and southwest) in Malaysia [27].

To conduct the experimental study, three reduced-scale models of the two-sided windcatcher with different ASCD angles were created. The models were made from Plexiglas with a thickness of 5 mm. The Plexiglas sheets were cut by laser with accuracy of 0.001 mm. As shown in

Fig. 2 (a), the three reduced-scale models were located above a rectangular cuboid with 600 mm length, 400 mm width and 300 mm height (representing a small class room). The room used in the analysis did not include window openings. It should be noted that previous work by [29] already carried out detailed analysis on performance of windcatchers assisted with windows. It is Since wing walls can be effective to improve ventilation in situations with low wind speed such as Malaysia [28]; thus, the windcatcher was integrated with wing walls with angle of 20°. However, studying the effect of this integration is out of the scope of this research and will be assessed in the future study presented by authors.

The windcatcher consisted of two channels which were separated with internal partition wall with 5 mm thickness. The heights of windcatcher and wing walls were 150 mm. The justification for the height selection is the fact that the height of traditional windcatchers are mostly between 1.5 m to 3 m and modern windcatchers are shorter than traditional ones for better adoption with current buildings [30]. The size of openings and cross-sections of windcatcher were 100 mm by 100 mm. The justification of the size of opening was based on typical size as described in the references [31]. The models with ASCD were similar but with different angle of 30°, 60° and 90° (angle of β in

Fig. 2 (b)).

(a) Scaled models with ASCD in the wind tunnel (from left to right β=90°, β =60° and β = 30°).

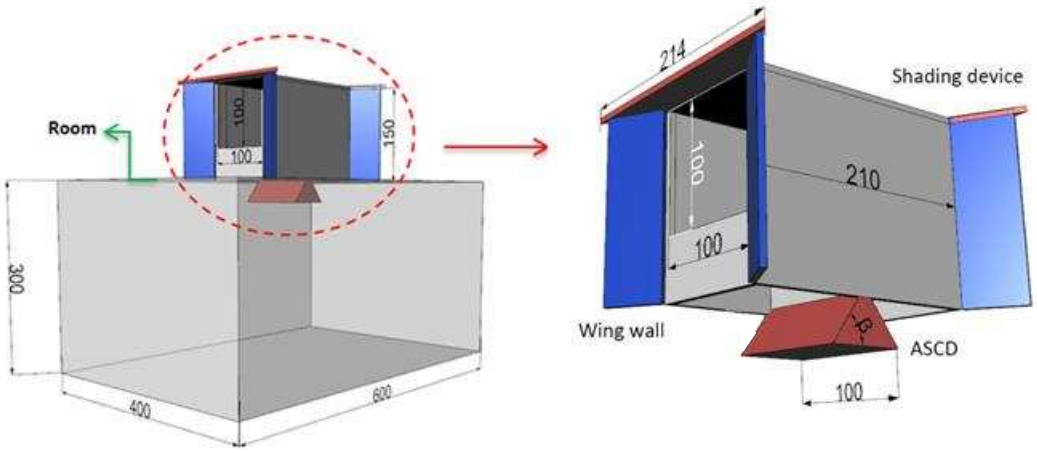

(b) The dimension of models with different angle of β

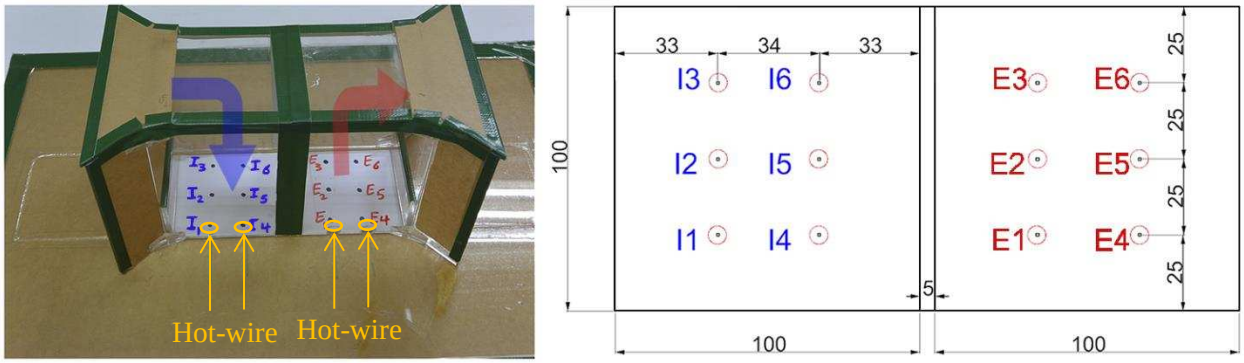

(c) The positions of I and E points in inlet and outlet

Fig. 2. (a) The three scaled models with ASCD in the wind tunnel (from left to right β=90°, β =60° and β = 30°),

(b) The dimension of models with different angle of β, (c) The positions of I and E points in inlet and outlet diffuser of models (all the dimensions are in mm).

The experiment was conducted in the Low Speed Wind Tunnel (UTM-LST) of University Technology Malaysia (UTM) which is a closed-circuit, horizontal return wind tunnel with a rectangular test section of 2 m (W) * 1.5 m (H) * 5.8 m (L). Based on the wind data of Malaysia, the predominant directions of the wind are northeast and southwest with an average of 2.5 m/s [27], [32] and [33]. Therefore, with respect to scale number of 1:10, the wind speed in wind tunnel should be set to 25 m/s to achieve the same Reynolds number. However, due to safety and strength of models, the wind speed was adjusted to 10 m/s.

During the test, the air velocity was measured in six points (I_1-I_6) in inlet diffuser and six points (E_1-E_2) in outlet diffuser (

Fig. 2 (c)). In order to locate the sensor inside the inlet diffuser channel, two holes (slightly larger diameter than the hot-wire sensor) were drilled on one side of the windcatcher as shown in Fig. 2 (c) (see orange arrows). The hot-wire sensor can traverse inside the channel to re-position between points. Similarly, two holes were also drilled on the outlet diffuser side to measure the exhaust flow velocities. The test consisted of 12 steps of data recoding for each model (totally 36). Points (I_1-I_6) and (E_1-E_2) are positioned in a symmetric grid in a horizontal plane (parallel to roof) in supply and exhaust channel. For each point, the measurement was done in Z vertical direction (parallel to channel) with duration of 1 minute which was repeated 3 times to have a more reliable data.

The method used for air velocity measurement was Constant Temperature Anemometry (CTA). The air velocity data logger utilized in this investigation was an OMEGA® HHF-SD1 combination standard thermistor anemometer and a hot wire which had multiple features that was required in this study. The OMEGA® HHF-SD1 had an accuracy of 5% of reading and resolution of 0.01 m/s. The hot wire sensor had 4 µm diameter, 1.27 mm long and can measure mean and fluctuating velocities in one-dimensional flows.

2.2 Computational Fluid Dynamics (CFD) modelling

The CFD simulation consisted of two phases. First phase was conducted for the validation of numerical method. In this phase, the computational domain and boundary conditions were selected to replicate the actual experimental conditions. A uniform flow wind speed of 10m/s was used for this analysis. Three models were simulated: windcatcher with 30°, 60° and 90° ASCD. In the second phase, an atmospheric boundary layer (ABL) flow model was used to investigate the performance of the windcatcher with ASCD in terms of airflow distribution, short-circuiting, supply rates and IAQ.

The computational domain used in this study for simulating ABL flows around different types of windcatcher configurations is illustrated in Fig. 3 (a). The domain size and location of model were based on the guideline of COST 732 [34] for environmental wind flow studies. The COST 732 suggested that for a single building with height of H, the lateral extension of the domain should be 5H (the distance between building's sidewalls and the lateral boundaries of the computational domain). For extension of the domain in flow direction, 5H was recommended for inlet. For the outlet, the boundary should be positioned at least 15H behind the building to allow the flow to re-develop behind the wake region, as fully developed flow is normally assumed as the boundary condition in steady RANS calculations. For the vertical extension of the domain, COST 732 advised between 4H and 10H with considering the effect of blockage [34]; So, to minimize the blockage, 10H was selected.

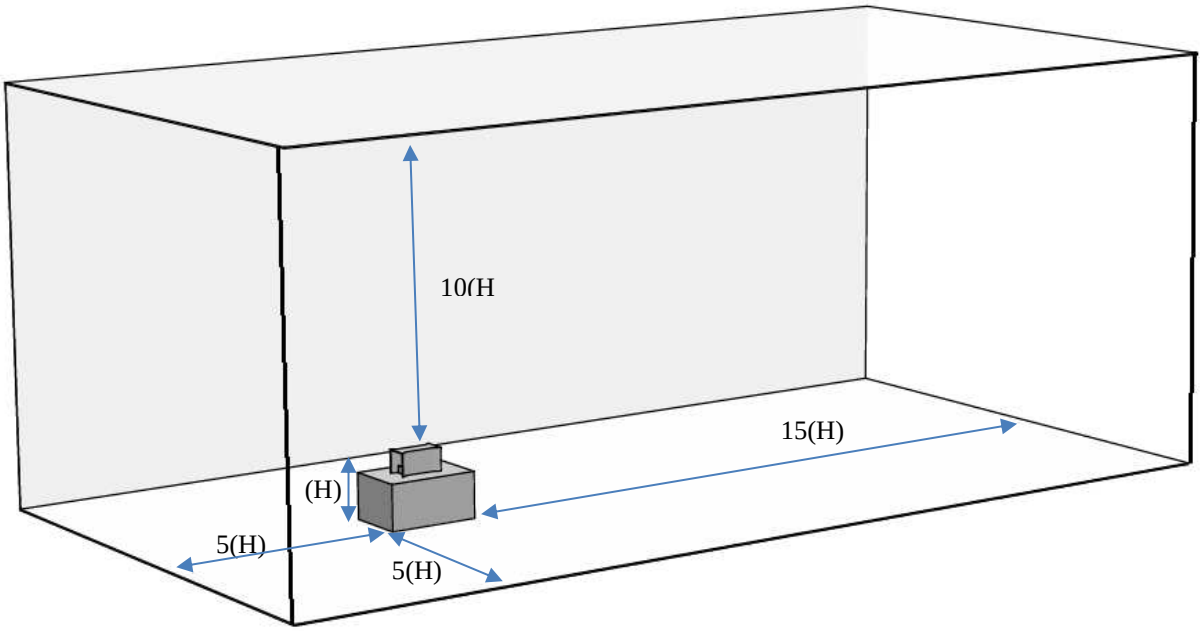

(a) Domain for the ABL flow

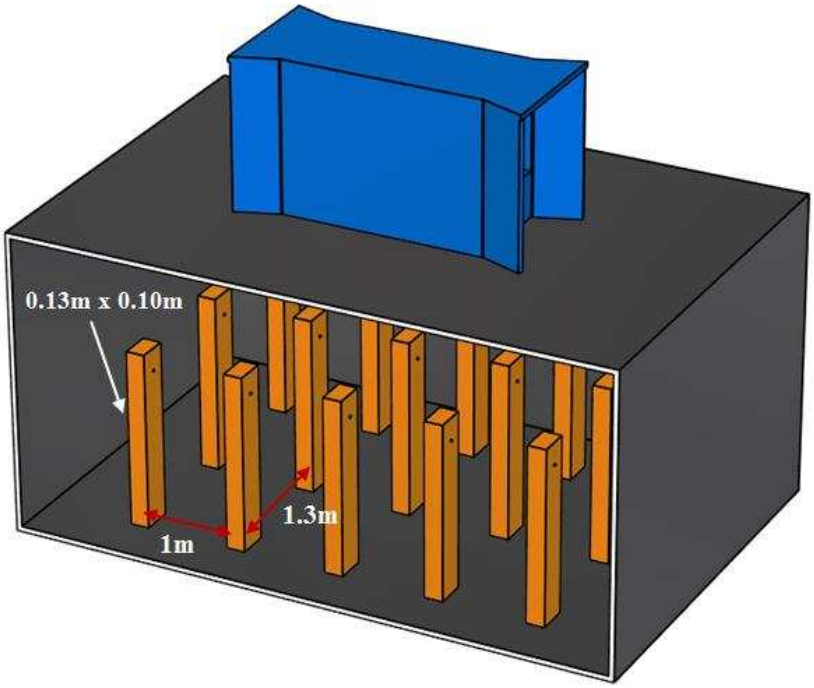

(b) Internal domain for the CO_2 analysis

Fig. 3. (a) The computational domain for the ABL flow simulations, (b) Internal domain for the CO_2 distribution simulation.

The study will also investigate the effect of the addition of the ASCD on the indoor CO_2 concentration, which will also be used identify the airflow short-circuiting inside the windcatcher. For the CO_2 distribution simulation, the room was filled with 15 occupants (equally distributed inside the room) as shown in Fig. 3 (b). The simplified exhalation (constant exhalation) model proposed by [19, 35] was used for the CO_2 distribution analysis. The model of the occupant was simplified to a 1.80m x 0.30m x 0.17m cuboid shape. The area for the mouth opening is equal to 0.13m x 0.10m. Average value of 6l/min of exhaled air was assumed for the simulation [19, 35]. The spacing of the occupants was based on reference [19]. The air was modelled as an incompressible fluid consisting of the species: oxygen (O_2), carbon dioxide (CO_2) and water steam (H_2O).

$$\frac{\partial(\rho Y_{O_2})}{\partial t} + \nabla \cdot \left(\rho Y_{O_2} u\right) = -\nabla \cdot j_{O_2} \qquad \text{(Equation 1)}$$

$$\frac{\partial(\rho Y_{O_2})}{\partial t} + \nabla \cdot \left(\rho Y_{O_2} u\right) = -\nabla \cdot j_{O_2} \qquad \text{(Equation 2)}$$

$$\frac{\partial(\rho Y_{O_2})}{\partial t} + \nabla \cdot \left(\rho Y_{O_2} u\right) = -\nabla \cdot j_{O_2} \qquad \text{(Equation 3)}$$

where ρ is density of fluid, t is time and u refers to fluid velocity vector and Y_i is mass fraction of i-th air constituent. The governing equations for continuity, momentum and energy conservation were not included here but can be found in the ANSYS 14.5 Fluent theory guide [36]. The comparison of the simplified exhalation model used in this study with results of [35] is detailed in Fig. A1.

The three-dimensional and steady Reynolds-Averaged Navier-Stokes (RANS) computations were performed using the commercial CFD code FLUENT 14.5 to solve the flow equations. The computational model employed the control volume method and the Semi-Implicit Method for Pressure-Linked Equations (SIMPLE) velocity-pressure coupling algorithm with the second order upwind discretization. Based on the turbulence model analysis, the standard k- ε model was used as the turbulence model (see the details in section 3.2.4.2). The use of the standard k- ε model on natural ventilation studies was also found in previous works of [16] and [18] to be

reliable and accurate. The governing equations for k- ε turbulence were not included here but can be found in the ANSYS 14.5 Fluent theory guide [36].

2.2.1 Mesh generation

The computational volumes were applied with non-uniform mesh due to the complexity of the geometry shape. The meshed model comprised of 1.5 mil nodes and 8.5 mil elements. The mesh around the windcatcher and openings were refined to ensure that the flow field was accurately captured in the simulations. The mesh was based on a grid sensitivity and flux balance analysis that will be described in Section 2.2.2.

2.2.2 Solution convergence and flux balance

There are no common metrics for deciding solution convergence. Residuals that are useful for one type of simulation are sometimes misrepresentative for other types of simulations. Therefore it is important to decide solution convergence not only by investigative residual levels, but also by monitoring relevant variables [36]. In this study, the convergence of the solution and relevant variables such as inflow and outflow velocities were monitored and the solution was completed when there were no changes between iterations. In addition to monitoring residuals and solution variables, the property conservation was also checked if achieved. This was carried out by performing a mass flux balance for the converged solution. This option was available in the FLUENT flux report panel which allows computation of mass flow rate for boundary zones. For the simulation of windcatcher, the mass flow rate balance was below the required value or <1% of smallest flux through domain boundary (inlet and outlet).

2.2.3 Boundary conditions

The boundary conditions were specified according to guidelines of AIJ [37] and COST 732 [34]. The profiles of the airflow velocity U and turbulent kinetic energy k were imposed at the inlet which were based on [38], with the streamwise velocity of the approaching flow obeying the power law with an exponent of 0.25 which corresponds to a sub-urban terrain. The velocity at H was 1.54m/s. The values of ε for the k-epsilon turbulence models were acquired by assuming local equilibrium of $P_k = \varepsilon$ [34]. The standard wall functions [39] were applied to the wall boundaries except for the bottom wall or ground, which had its wall functions adjusted for roughness [40]. According to [40], this should be specified by an equivalent sand-grain roughness height k_s and a roughness constant C_s. The horizontal non homogeneity of the ABL

was limited by adapting sand-grain roughness height and roughness constant to the inlet profiles, following the equation of [41]:

$$k_s = \frac{9.793 z_0}{c_s} \quad \text{(Equation 4)}$$

Where z_0 is the aerodynamic roughness length of the sub-urban terrain. The values selected for sand-grain roughness height and a roughness constant 1.0 mm and 1.0 [38]. The sides and the top of the domain were established as symmetry boundary conditions, indicating zero normal velocity and zero gradients for all the variables at the side ant top wall. At the outlet boundary wall, zero static pressure was used. Summary of the boundary conditions are shown in Table 1 and Table 2. The comparison of our results with [38] is presented in the Appendix section.

Table 1 Summary of boundary conditions for the domain

Parameter	Domain
Micro-Climate	Fluid zone
Walls	Top: Symmetry Side: Symmetry Bottom: Wall
Macro-climate	Fluid zone
Operating Pressure	Atmospheric
Viscous Model	k- ε (standard)
Near-Wall Treatment	Standard wall functions
Velocity Inlet	ABL Profile
Pressure Outlet	0 Pa
Solver Type	Pressure-based
Time	Steady

Table 2 Boundary conditions for the CO_2 simulation.

Human body dimension	1.80 x 0.30 x 0.17 m^3 [19, 35]
Number of occupants	15

Mouth dimension	0.13 x 0.1 m^2 [35]
Exhaled air	6 l/min (0.77 m/s) [35]
Inlet CO_2 concentration	382 ppm [35]
Exhaled air CO_2 concentration	36,000 ppm [35]

2.2.4 Sensitivity analysis

3.2.4.1 Grid adaption

In order to ensure that the numerical model was independent from the grid size, different number of grids were evaluated (4, 8 and 12 million elements). The computational mesh was based on a mesh sensitivity analysis which was performed by conducting additional simulations with same domain and boundary conditions but with various mesh sizes. The area-weighted average value of the inflow velocity in the vertical height of the room was taken as the error indicator (Fig. 4), as the grid was refined from coarse 4 million to fine 12 million elements. The maxim error between the fine and medium size mesh was obtained at height of 2.8m which was 2.1% which was equivalent to ±0.015m/s. Thus, the repetition of numerical model with finer mesh had no considerable effects on the results. Consequently, using the mentioned mesh size was sufficiently accurate and no need for the finer mesh.

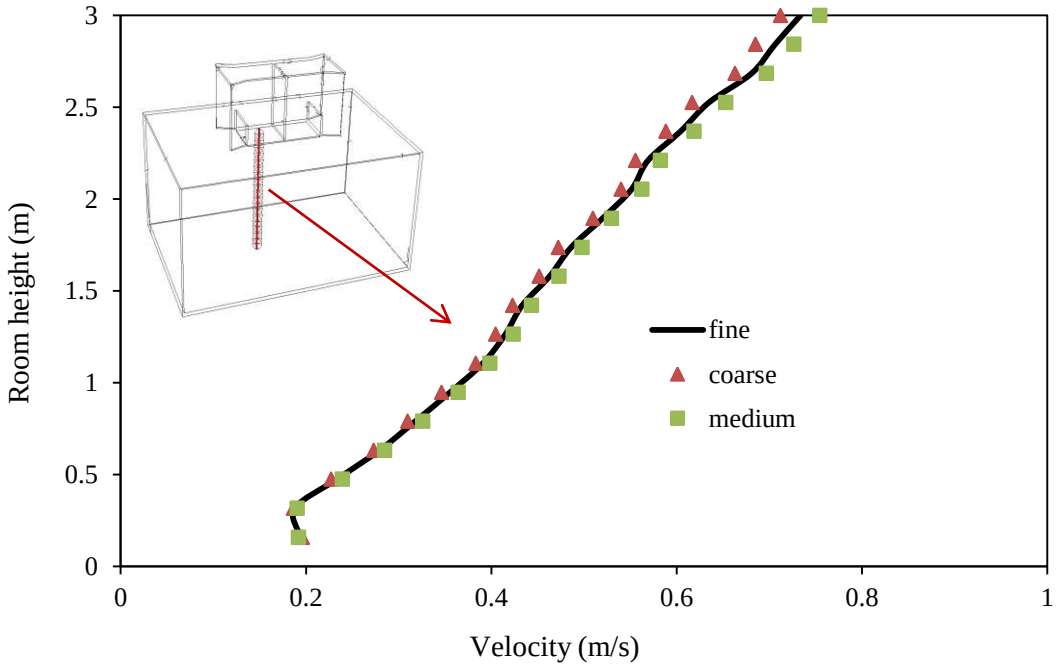

Fig. 4. Grid sensitivity analysis of different sizes: 4million (coarse), 8million (medium) and 12 million (fine).

3.2.4.2 Sensitivity of turbulence model

Turbulence model validation is a fundamental importance for the reliability of CFD simulations. The objective of turbulence sensitivity analysis was to verify that the selected turbulence model was able to present the most accurate prediction of the flow. For this reason, three turbulence models were evaluated including (1) the standard k-ε (Sk-ε) model, (2) the realizable k-ε (Rk-ε) model and (3) the renormalization group k-ε model (RNG k-ε). The predictions of the three different turbulence models on the airflow velocity in I and E points of inlet and outlet channels of windcatcher with 30° ASCD are presented in Table 3. The standard k-ε model clearly provided the best agreement with the experimental data. The average of difference between experimental data and mentioned model was 9.3% (lower than the other two models). Therefore, standard k-ε model was selected for current numerical study which was in agreement with pervious windcatcher studies in reference of [16] and [18].

Table 3 The air velocity (m/s) results of turbulence sensitivity analysis for windcatcher with 60° ASCD.

Point	Experiment	Sk-ε	RNG k-ε	Rk-ε
i1	3.40 m/s	4.00 m/s	3.15 m/s	2.70 m/s
i2	4.90 m/s	4.50 m/s	3.59 m/s	3.02 m/s
i3	4.90 m/s	4.20 m/s	4.05 m/s	2.70 m/s
i4	6.40 m/s	6.65 m/s	5.84 m/s	6.75 m/s
i5	6.70 m/s	6.80 m/s	5.84 m/s	6.75 m/s
i6	6.50 m/s	6.65 m/s	5.4 m/s	6.75 m/s
e1	5.90 m/s	5.90 m/s	5.84 m/s	5.85 m/s
e2	5.60 m/s	5.50 m/s	7.65 m/s	4.92 m/s
e3	5.80 m/s	5.60 m/s	5.40 m/s	5.85 m/s
e4	6.40 m/s	6.50 m/s	6.30 m/s	6.75 m/s
e5	6.40 m/s	6.50 m/s	7.19 m/s	6.30 m/s
e6	6.70 m/s	6.50 m/s	7.19 m/s	6.75 m/s
Average of difference with experiment		**9.30%**	**12.00%**	**11.09%**

3 Results and discussion

3.1 CFD validation with wind tunnel measurements

To validate the numerical method, the CFD results were compared against the experimental data obtained from wind tunnel testing of three scaled models. Fig. 5 (a), (b) and (c) demonstrate the air velocity results obtained from experimental test and CFD simulation (measured in points I_1-E_6 in

Fig. 2 (c)) related to the windcatchers with 60°, 30° and 90° ASCD. The average error were 6.82% for the windcatcher with 30° ASCD, 9.3% for the 60° ASCD and 6% for the 90° ASCD. Hence, it can be established that the simulation agreed with experimental data and validated. Most of the measurements and CFD data were in good agreement except for point e2 in the windcatcher with 30° ASCD. This is probably due to the turbulence model standard k-epsilon which is limited in terms of predicting complex flows such as flow separations. This complex flows can be observed in Figure 7b in the exhaust channel of the windcatcher.

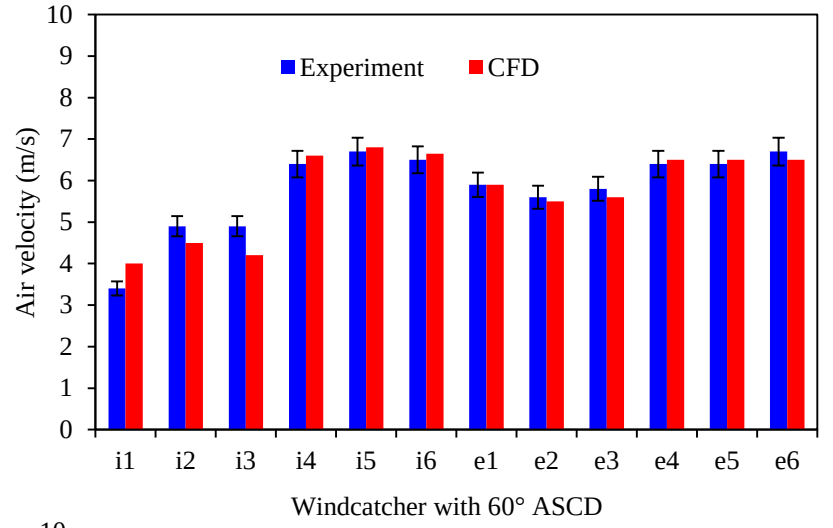

Windcatcher with 60° ASCD

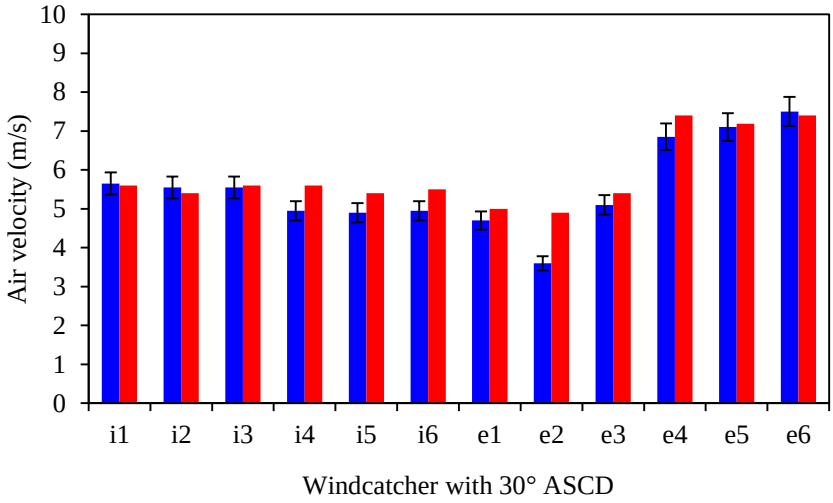

Windcatcher with 30° ASCD

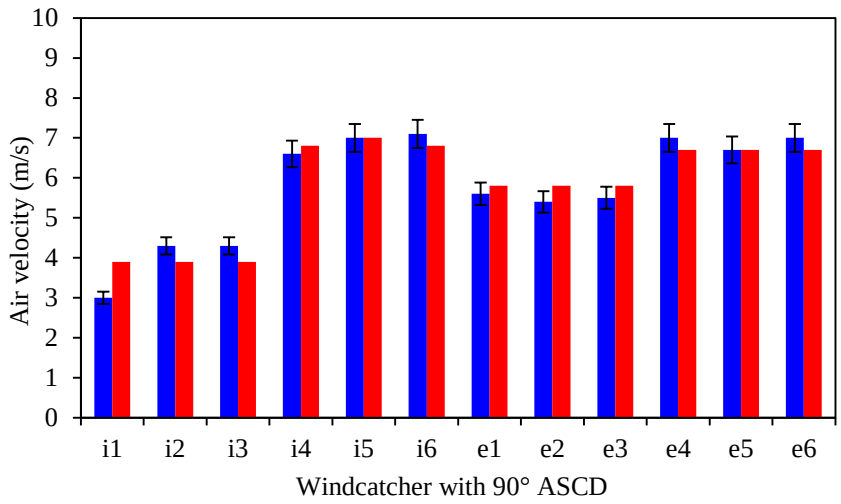

Fig. 5. Comparison between experimental and simulation results for windcatcher with 60°, 30° and 90° ASCD. Errors bars with 5% value.

3.2 CFD simulation results

3.2.1 Overall airflow velocity analysis

Fig. 6 (up) shows the velocity contours of a cross-sectional plane inside the computational domain representing the airflow distribution inside the room with the two-sided windcatcher without ASCD (reference case). As observed, the approach wind profile entered from the left side of the domain and the airflow slowed down as it approached the building and lifted up. Separation zones were observed on the front side of the building and front edge of the roof which affected the airflow entering the windcatcher. The airflow inside the supply of the windcatcher was re-directed downwards when it hit the partition wall, causing the airflow to speed up near the partition wall reaching up to 1.2 m/s. The airflow induced inside the room spread as it reached the floor causing airflow recirculation on all sides. The airflow was recirculated inside the room and exited the space through the exhaust channel of the windcatcher; this was aided by the large airflow re-circulation generated at the back of the windcatcher and building model. The airflow short-circuiting effect was not very clear from the velocity contours hence, it will be analyzed separately in Section 4.2.3. Likewise, Fig. 6 (down) shows the analysis of the velocity contours in and around the windcatcher with a 30° ASCD. It was clear that a similar pattern was observed until the diffuser section of the windcatcher where the airflow was directed towards the left corner of the room.

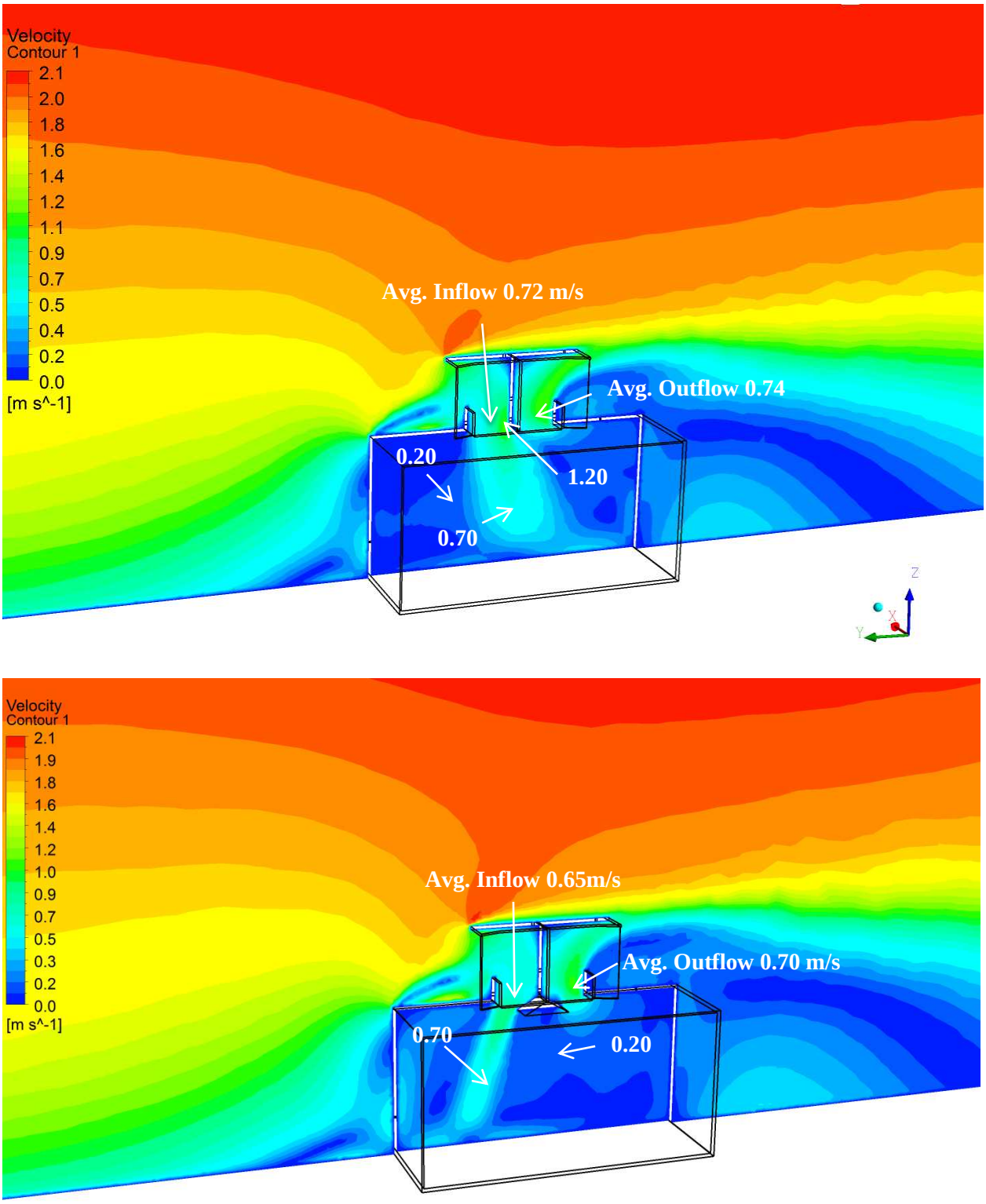

Fig. 6. Air velocity contours in windcatcher without ASCD (up) and with 30° ASCD (down).

3.2.2 Airflow short-circuiting analysis

Short-circuiting of ventilation air occurs when ventilation air enters and leaves a space or duct before it has a chance to mix well enough with room air to do the job it was intended to do which is to adequately dilute indoor pollutants. Short-circuiting of ventilation air can occur for any system where air is supplied in close proximity to where air is returned. Where outlet or inlet placement does not allow for much separation as observed in Fig. 7 (a). Nevertheless, Fig. 7 (b) proves that the ASCD can prevent or reduce the short-circuit phenomenon by re-directing the supply air away from the exhaust stream.

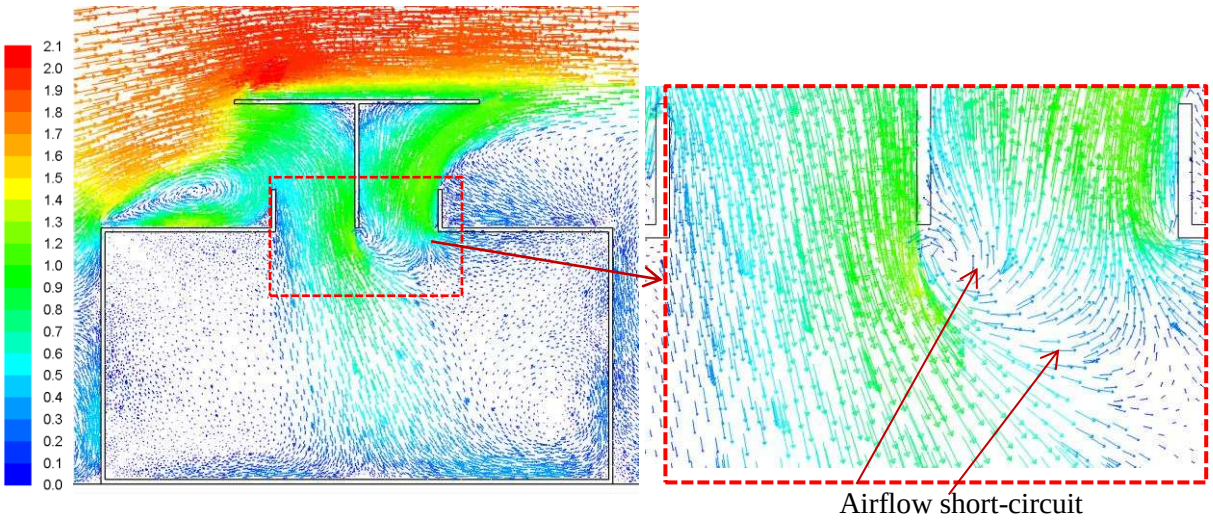

(a) reference windcatcher (without ASCD).

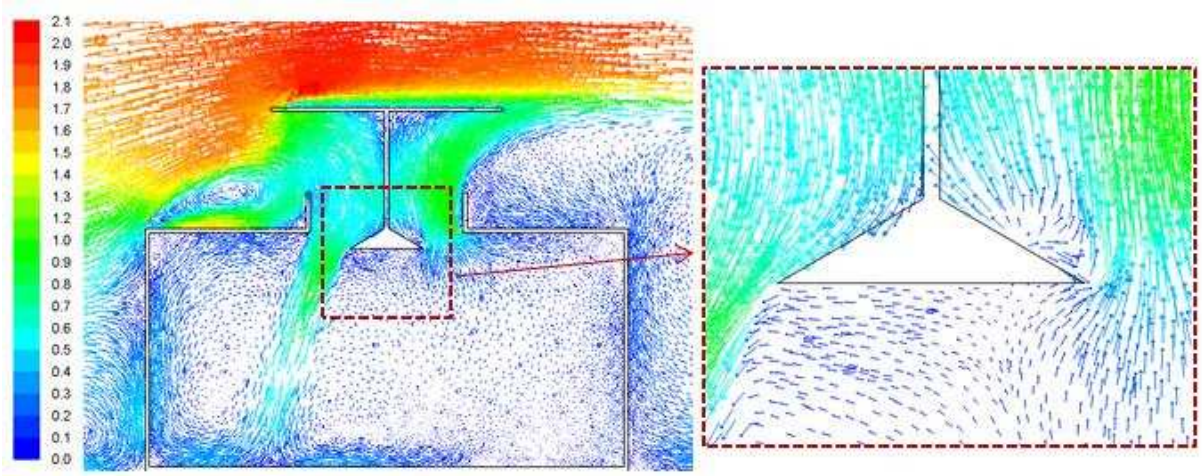

(b) windcatcher with 30° ASCD

Fig. 7. Velocity vectors of mid-plane inside the domain with reference windcatcher (a) and windcatcher with 30° ASCD (b).

The red dashed line in Fig. 8 denotes the airflow crossing the green plane (1.5m (H) x 1m (L)) towards the exhaust side of the windcatcher. In this study, this plane was used to quantify the airflow (y-velocity) that enters the exhaust stream instead of entering the space. The blue and red planes are used to measure the average speed inside the supply and exhaust channels to investigate the effect of the addition of ASCD on the supply and exhaust rates. The yellow plane is used to plot the airflow distribution inside the space.

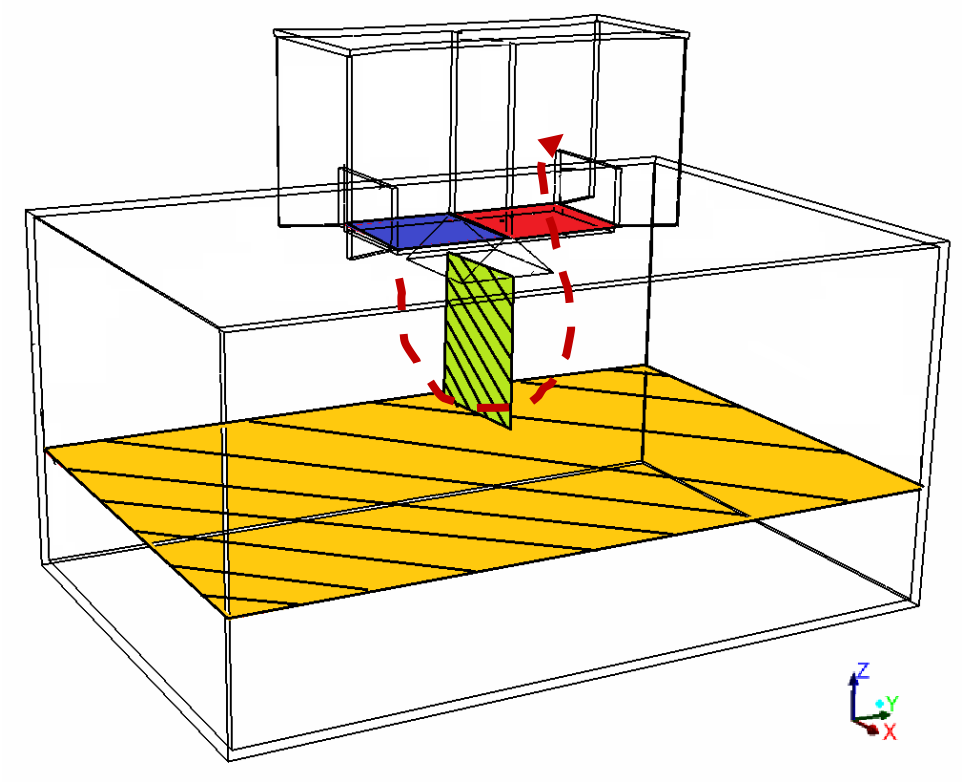

Fig. 8. Measurement planes for inflow (blue), outflow (red), air short-circuit (green) and indoor airflow distribution (yellow).

The Fig. 9 shows the averaged velocity and direction of the air flow inside the green plane; a positive value indicates the supply stream airflow crossing the plane and entering the exhaust region, while a negative value indicates the exhaust stream crossing the plane and entering the supply region. The middle line or the zero value indicates that supply stream does not enter the exhaust area and exhaust stream does not enter the supply area. The results indicated that all the

ASCD was able to keep the supply airflow stream in the supply area (left region) except for the 90° ASCD, however it was minimal and very close to the middle line. Without the ASCD, the airflow supply stream enters the exhaust region at a higher average speed (0.26 m/s).

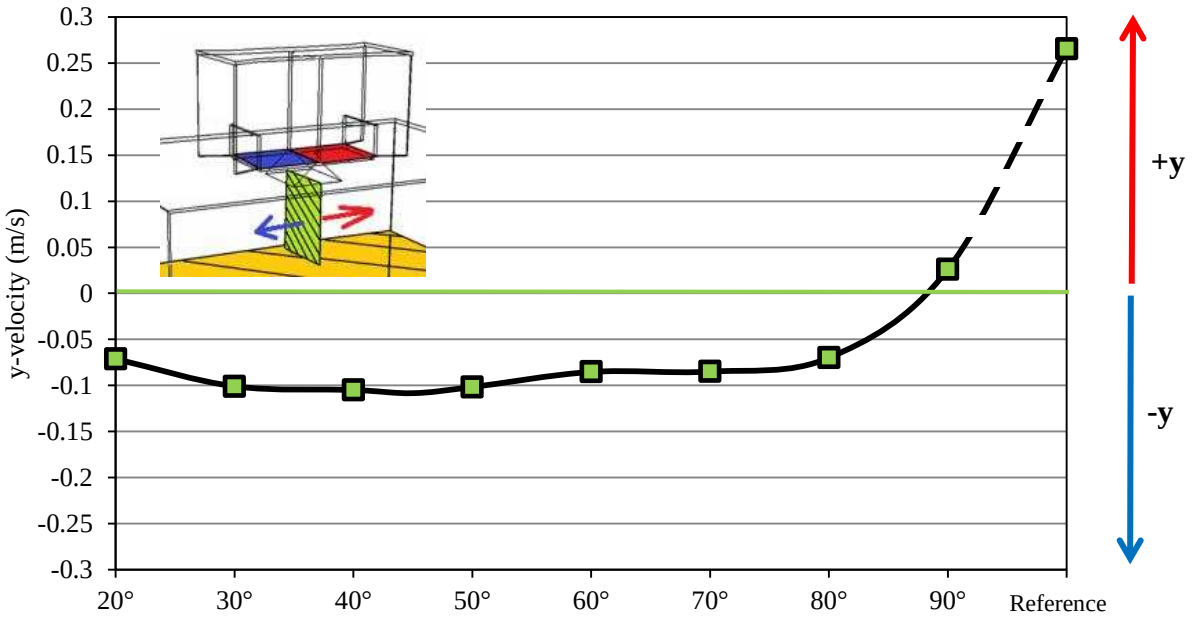

Fig. 9. The averaged velocity and direction of air flow inside green plane in windcatchers with ASCD (in different angle) and the reference windcatcher.

3.2.3 Supply rates as a prominent IAQ parameter

Air flow rate is an important factor for IAQ analysis since most of the standards suggest the minimum requirement based on this factor. In Fig. 10, it can be observed windcatcher with ASCD had more air speed (averaged) in the supply than the reference case in high angles (60° to 90°) but the ASCD slightly lowers the speed of the airflow at lower angles. This is because at lower angles, the ASCD blocks a larger area of the diffuser of the windcatcher. The maximum velocity, which occurred at 90°, was 6% more than reference case and 20% more than the minimum (20°). Hence, beside the short-circuit reduction, the higher angle ASCDs also improved the air supply rate.

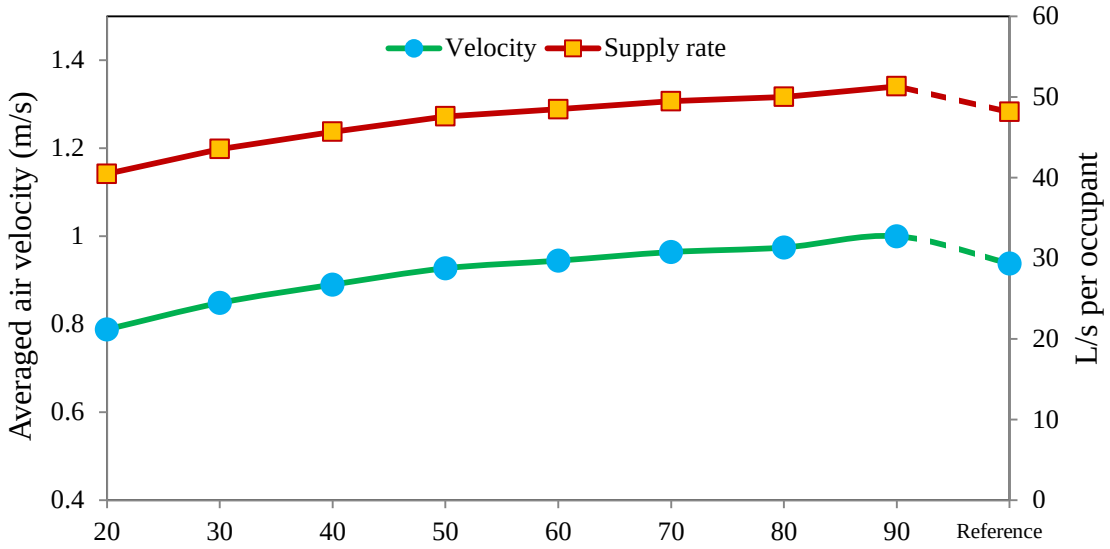

Fig. 10. The averaged air velocity (in diffusers) and supply rate of fresh air of windcatchers with ASCD (in different angles) and the reference windcatcher.

Moreover, Fig. 10 illustrates the calculated supply rates of the windcatcher with and without ASCD. The calculation was based on the room with 15 occupants and wind speed of 2.5m/s. As observed, all configuration was able to supply more than 40 l/s per occupant which is higher than ASHRAE 62 and BS5925:1991 minimum requirement for indoor environment of educational space [42]. ASCDs with high angle (60° to 90°) could supply more fresh air than the reference case. Comparing ASCD windcatcher with other windcatchers assessed in previous studies can reveal its better performance over them. For instance, Hughes and Ghani [21] in their studied evaluated a 1mx1m commercial four-sided windcatcher in different wind speeds with same dimension as this study. The maximum supply rate, which they achieved, was 32 L/s/occupant but at 5 m/s wind speed. Consequently, windcatcher with ASCD was able to provide 60% more fresh air than the commercial one but in two times less wind speed which proves its higher ventilation efficiency. Likewise, in other study conducted by Calautit and Hughes [6], their 1mx1m commercial windcatcher could produce 27 l/s/occupant at 3 m/s wind speed in approximately same size classroom which was also nearly two times less than the windcatcher in this study.

3.2.4 Indoor airflow analysis

The airflow jet was slight offset toward the left region of the room with 30° and 60° ASCD windcatcher and therefore greater airflow speed was observed in the left region as shown in Fig. 11. Two horizontal planes (similar to yellow plane in Fig. 8) were used to plot the contours: breathing height at sitting position (1m) and standing position (1.7m) with respect to ASHRAE55 standard recommendations [43]. For the sitting height (Fig. 11), it can be observed that the addition of ASCD improved the airflow distribution and a slightly higher average speed was calculated for the ASCD configurations. It can be observed that the dark blue spots or airflow <0.1m/s was less for the ASCD models as compared to the base model. Similar observation was made for the contours at standing height in Fig. 12, except for the 90° ASCD which had higher airflow.

In addition, the minimum average of air velocity of 1m sitting plane in the room (Fig. 11) with ASCD windcatcher was seen in 30° ASCD with 0.167m/s which was 19% higher than reference windcatcher. But the maximum was 60° with 0.18m/s which increased 28% than the reference windcatcher (without ASCD). However, the minimum and maximum differences with reference case for 1.7m standing plane were 27% to 37% belonged to 30° and 60° respectively.

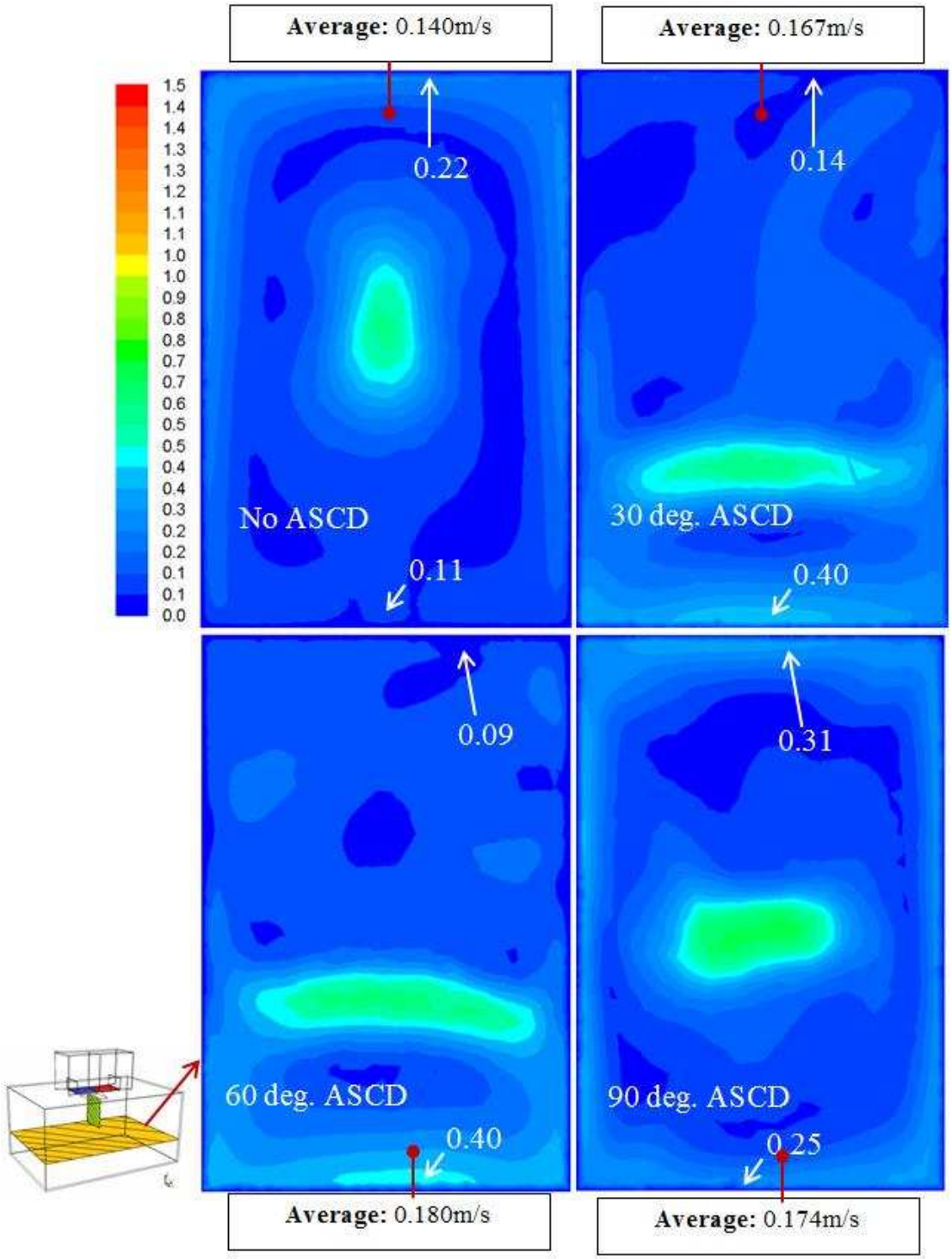

Fig. 11. Velocity contours of mid-plane (1 m) at sitting breathing height with windcatcher with and without ASCD.

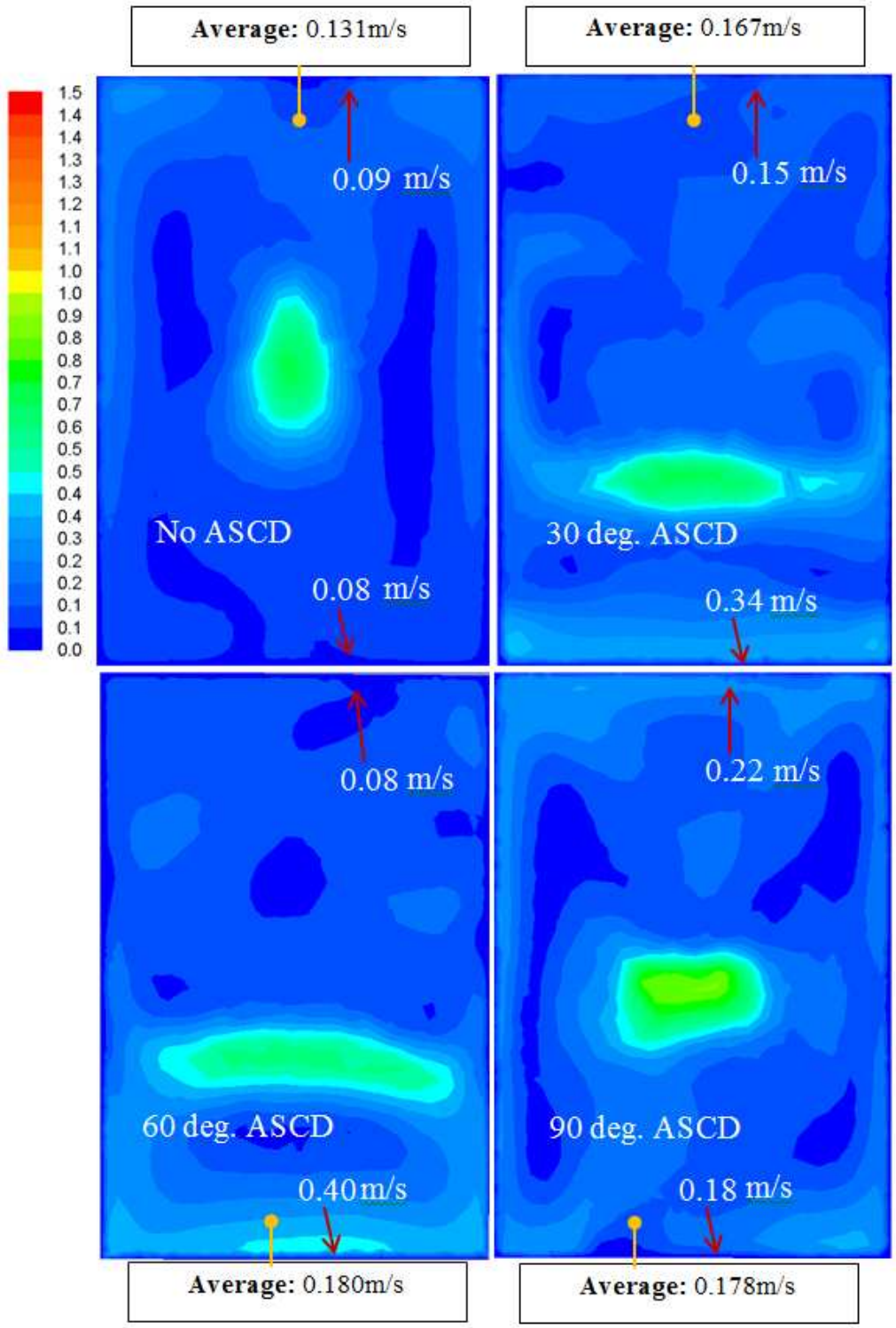

Fig. 12. Air velocity contours of mid-plane (1.7m) at standing breathing height with windcatcher with and without ASCD.

3.2.5 Indoor air quality analysis

Windcatcher with 30° ASCD

Fig. 13 shows the CO_2 distribution contours of the cross-sectional plot drawn from the middle of the room with 15 occupants. In the simulation, the occupants were assumed to be the source of carbon dioxide. As observed in Windcatcher with 30° ASCD

Fig. 13 (a), the windcatcher supplied fresh air at 382ppm inside the room with most of it directed towards the central area. Some of the fresh air can be observed entering the exhaust stream of the windcatcher which indicates fresh air short-circuiting. In Windcatcher with 30° ASCD

Fig. 13 (b), the fresh airflow was re-directed towards the corner of the room and away from the exhaust stream. Corners of the room with ASCD windcatcher showed lower CO_2 concentration and a better overall CO_2 distribution was also observed.

Windcatcher with 30° ASCD

Fig. 13 (a) and Windcatcher with 30° ASCD

Fig. 13 (b) reveal that more homogenous fresh air distribution can be seen in the room with windcatcher with ASCD than the reference case. However, in the reference case the fresh air had the highest concentration in the middle of the room and occupants in the corners were more exposed to higher CO_2 concentration which proves the capability of ASCD to raise indoor air quality especially in educational space.

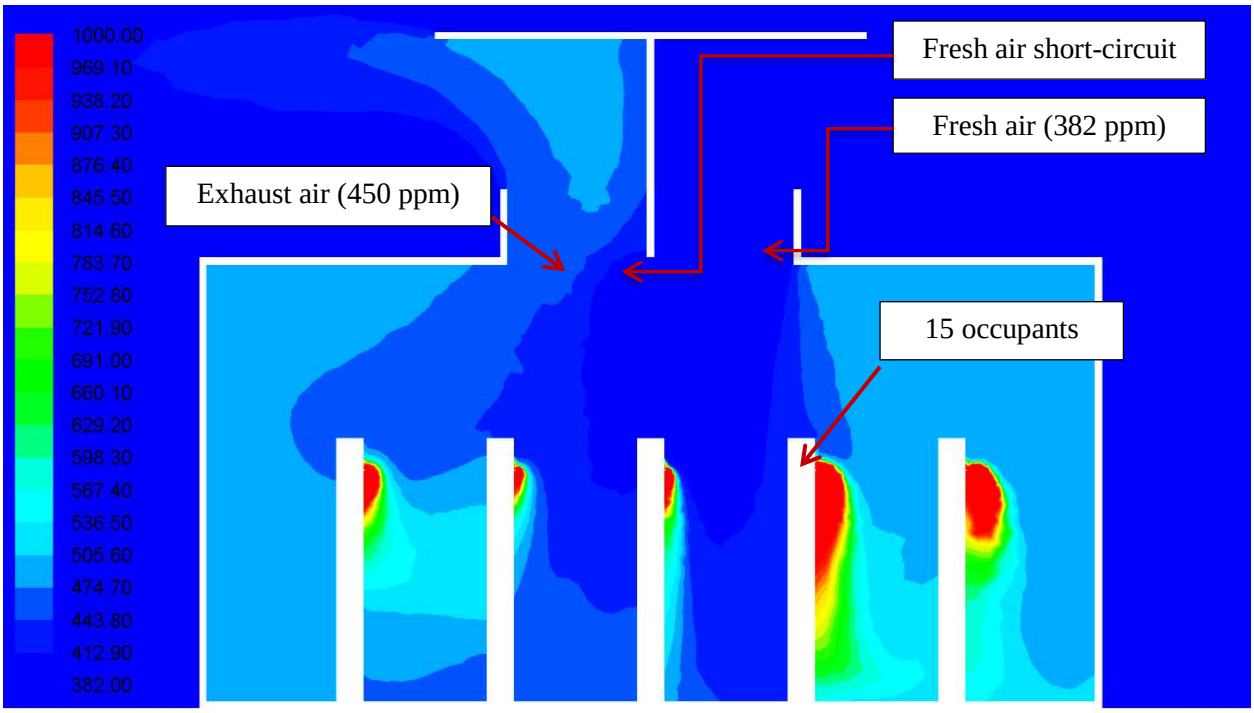

(a) The reference windcatcher.

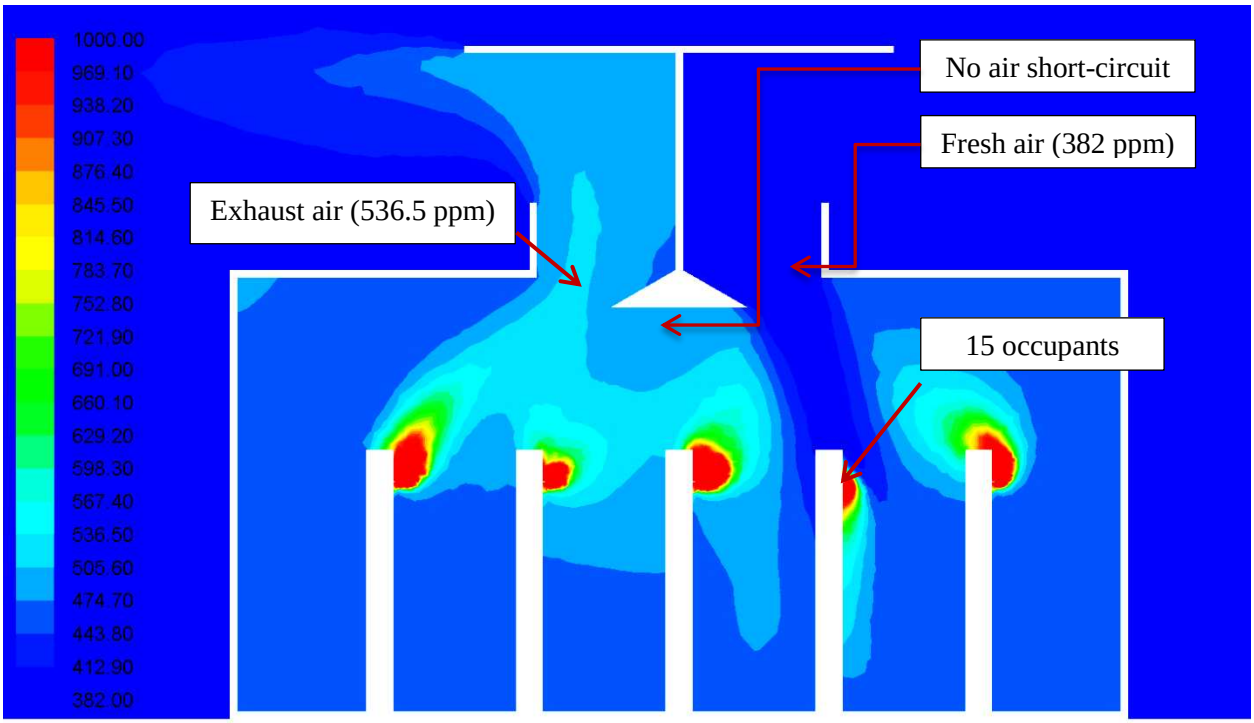

(b) Windcatcher with 30° ASCD

Fig. 13. (a) CO_2 analysis inside the room with the reference windcatcher, (b) CO_2 analysis inside the room with 30° ASCD windcatcher.

Fig. 14 shows the CO_2 distribution contours of the midplane drawn from the diffuser channel of the windcatcher. As observed, the supply channels for both windcatchers (with and without ASCD) were supplying fresh air at 382ppm. It is clear that the airflow exiting the exhaust channel of the windcatcher without ASCD had a lower CO_2 concentration as compare to the windcatcher with a 30° ASCD. This indicates that the addition of ASCD improved the circulation of the flow inside the room and also enhanced the extraction of stale air inside the room. It is also evident from Fig. 14 (left), that some of the fresh air from the supply was exiting the exhaust channel without entering the room.

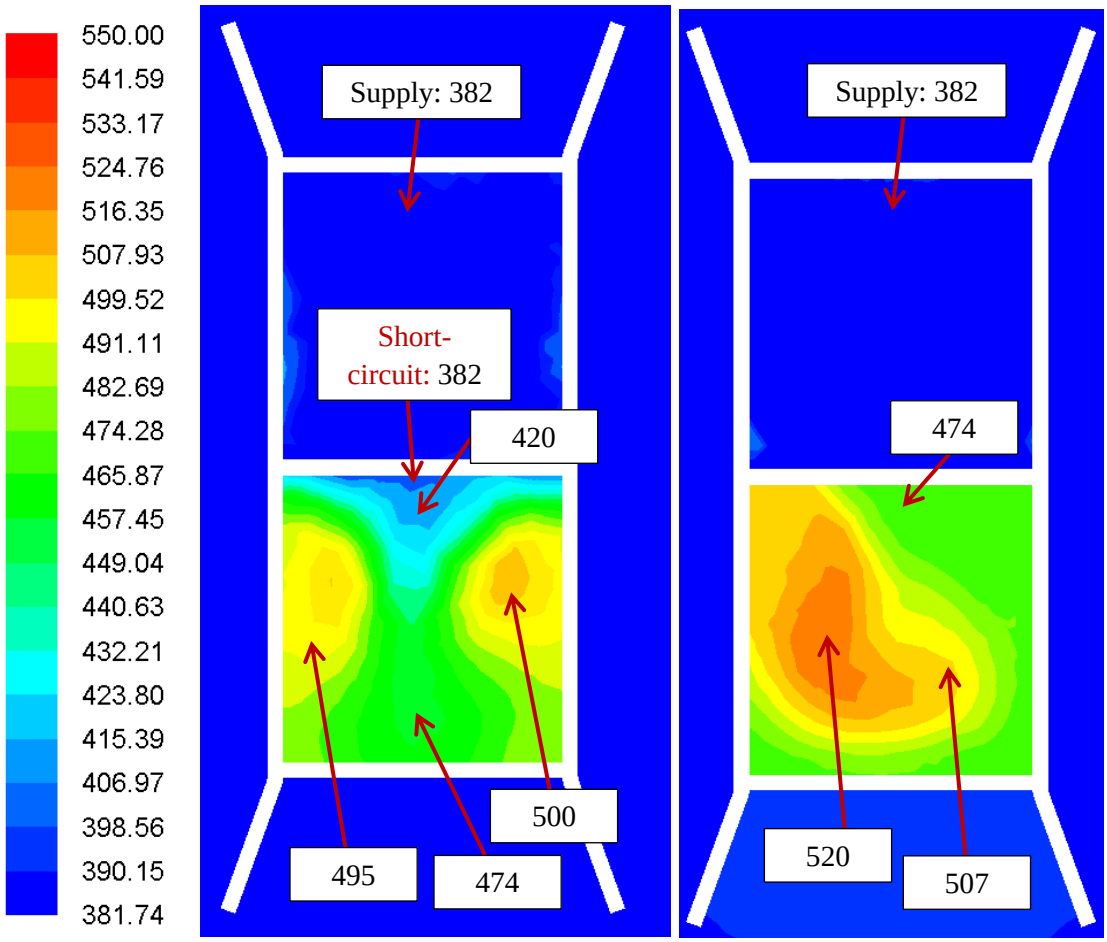

Fig. 14. CO_2 concentration contour in diffuser plane in windcahcer without ASCD (left) and with 30° ASCD (right).

Fig. 15 shows the CO_2 distribution contours at 1m (sitting height) and 1.7m (standing height) respectively. In the model, the occupants were assumed to be standing hence a higher

concentration was observed in the 1.7m contour. As observed, the 30° ASCD clearly lowered the average CO_2 concentration inside the room for both heights. The fresh air had more homogenous distribution with lower concentration in the room with ASCD windcatcher (b and d in Fig. 15). In addition, the average of CO_2 concentration was 40 PPM lower than reference case. Furthermore, very high CO_2 concentration (red spots) can be observed near heads of the students in the classroom with the reference windcatcher in Fig. 15 (c) except for those who were in the middle, but these hot spots were reduced considerably in classroom with 30° ASCD windcahcer (Fig. 15 (d)).

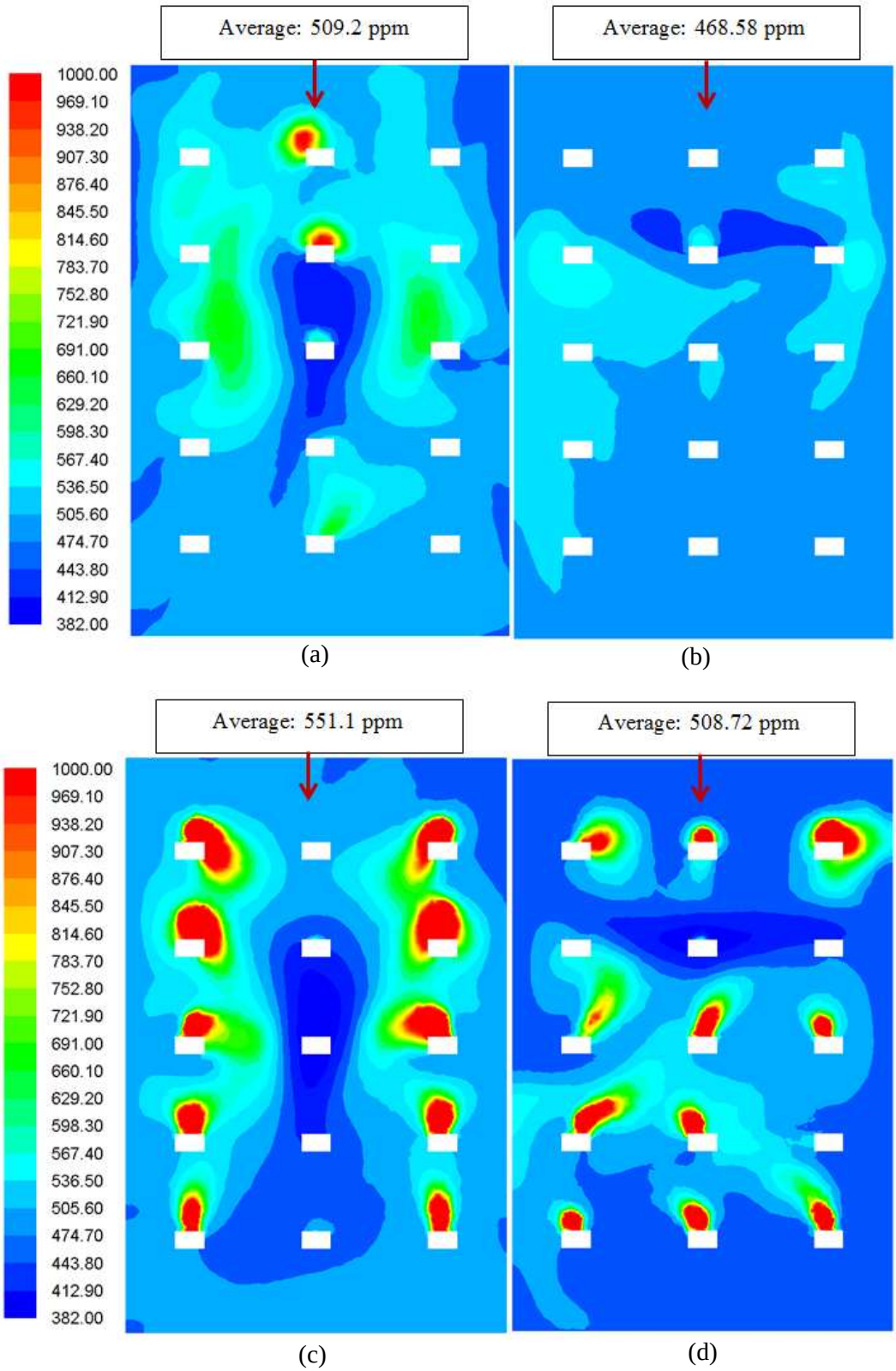

Fig. 15. CO_2 concentration contour in 1 m height plane in reference windcatcher (a) and windcahcer with 30° ASCD (b) and in 1.7 m height plane in reference windcatcher (c) and windcatcher with 30° ASCD (d).

4 Conclusion

The review of previous works on windcatchers showed that several authors have observed the short-circuiting effect in windcatchers but did not assess it or quantify it in details. This study presents several methods which can be used to assess this effect and also prevent it using anti short-circuit device (ASCD) which is a new windcatcher component acts such as a fin to direct the air flow in diffuser of windcatcher. The research consisted of experiment of reduced-scale models in wind tunnel and CFD simulation. The CFD modelling was validated using wind tunnel testing and good correlation was observed. The average errors for all the models were all below 10%. The study used atmospheric boundary layer (ABL) flows to simulate the ASCD windcatcher with various ASCD angle. The approach flow profile considered obeyed the power law with an exponent of 0.25 which corresponds to a sub-urban terrain. The simulated airflow speeds were based on low-wind speed conditions of Malaysia.

Different ASCD angles were examined by investigating the ventilation performance of the windcatcher with various angles (20º to 90º). It was found that the ASCD windcatcher with angles between 20°-80° prevented fresh air from entering the exhaust region. The addition of ASCD (20°-80°) showed that the fresh airflow was re-directed towards the corner of the room and away from the exhaust channel. The analysis also showed that lower ASCD angles (20°-40°) can slightly reduce the average airflow supply speed because the ASCD at lower angles blocks a large area of the diffuser. The calculation was based on a room with 15 occupants and wind speed of 2.5m/s. The velocity contour plots created at sitting and standing breathing heights with respect to ASHRAE55, to observe the overall airflow indoor distribution in windcatchers with ASCD and the reference windcatcher.

The CO_2 concentration analysis proved to be a useful indicator of short-circuiting in windcatchers. The reference windcatcher without ASCD showed that fresh air was directed towards middle of the room lowering the CO_2 concentration in this area but higher CO_2 concentration was observed in the left and right corners of the room, which was in agreement with the airflow distribution analysis. The CO_2 concentration in the exhaust of a windcatcher with ASCD was 20ppm higher, indicating that it was more effective in terms of removing stale air out of the room. In addition, the windcatcher without ASCD showed 8% higher CO2

concentration in the room indicating that ASCD was more effective in terms of removing stale air out of the room.

Likewise, the results demonstrated that the ASCD windcatcher (angles between 20°-80°) could supply from 40- 51 l/s per occupant which is significantly higher than the minimum requirement that recommended by ASHRAE62.2 and BS BS5925 standards. In addition, the average air velocity of 1 m height horizontal (sitting) plane in the room with ASCD windcatcher was 19% to 28% higher than reference windcatcher (without ASCD) while this increase for 1.7 m height horizontal (standing) plane was 27-37%. Therefore, it could be concluded that the addition of ASCD lowered the CO_2 concentration and improved the indoor air quality and simultaneously raised the ventilation performance of the windcatcher.

References

[1] L. Yang, H. Yan, J.C. Lam, Thermal comfort and building energy consumption implications – A review, Applied Energy. 115 (2014) 164–173. doi:10.1016/j.apenergy.2013.10.062.

[2] B. Chenari, J. Dias Carrilho, M. Gameiro da Silva, Towards sustainable, energy-efficient and healthy ventilation strategies in buildings: A review, Renewable and Sustainable Energy Reviews. 59 (2016) 1426–1447. doi:10.1016/j.rser.2016.01.074.

[3] T. Yu, P. Heiselberg, B. Lei, M. Pomianowski, C. Zhang, R. Jensen, Experimental investigation of cooling performance of a novel HVAC system combining natural ventilation with diffuse ceiling inlet and TABS, Energy and Buildings. 105 (2015) 165–177. doi:10.1016/j.enbuild.2015.07.039.

[4] M.C. Katafygiotou, D.K. Serghides, Thermal comfort of a typical secondary school building in Cyprus, Sustainable Cities and Society. 13 (2014) 303–312. doi:10.1016/j.scs.2014.03.004.

[5] H.M. Taleb, Natural Ventilation as Energy Efficient Solution for Achieving Low-Energy Houses in Dubai, Energy and Buildings. (2015). doi:10.1016/j.enbuild.2015.04.019.

[6] J.K. Calautit, B.R. Hughes, Wind tunnel and CFD study of the natural ventilation performance of a commercial multi-directional wind tower, Building and Environment. 80 (2014) 71–83. doi:10.1016/j.buildenv.2014.05.022.

[7] O. Saadatian, L.C. Haw, K. Sopian, M.Y. Sulaiman, Review of windcatcher technologies, Renewable and Sustainable Energy Reviews. 16 (2012) 1477–1495. doi:10.1016/j.rser.2011.11.037.

[8] H. Montazeri, Experimental and numerical study on natural ventilation performance of various multi-opening wind catchers, Building and Environment. 46 (2011) 370–378. doi:10.1016/j.buildenv.2010.07.031.

[9] C. Ionescu, T. Baracu, G.-E. Vlad, H. Necula, A. Badea, The historical evolution of the energy efficient buildings, Renewable and Sustainable Energy Reviews. 49 (2015) 243–253. doi:10.1016/j.rser.2015.04.062.

[10] Z. Komijani, A. Gharachorlou, F.Z. Ahari, M.B. Abadi, F. Nahidi, A.H.G. Zahra Komijani, Afshin Gharachorlou, F. Zargarian Ahari Maryam Batoomi Abadi1, F. Nahidi Azar, et al., Wind Catcher History and Performance in Iran as Iranian Ancient Architectural Heritage, NATIONALPARK-FORSCHUNG IN DER SCHWEIZ (Switzerland Research Park Journal). 103 (2014) 1343–1350. http://www.naukpublication.org/index.php/NATIONALPARK-FORSCHUNG-SCHWEIZ/article/view/538 (accessed December 16, 2014).

[11] A.R. Dehghani-sanij, M. Soltani, K. Raahemifar, A new design of wind tower for passive ventilation in buildings to reduce energy consumption in windy regions, Renewable and Sustainable Energy Reviews. 42 (2015) 182–195. doi:10.1016/j.rser.2014.10.018.

[12] M.N.N. Bahadori, M. Mazidi, a.R. Dehghani, A.R. Dehghani, Experimental investigation of new designs of wind towers, Renewable Energy. 33 (2008) 2273–2281. doi:10.1016/j.renene.2007.12.018.

[13] A.A. Elmualim, Integrated Building Management Systems for Sustainable Technologies: Design Aspiration and Operational Shortcoming, in: n.d.

[14] A.A. Elmualim, H.B. Awbi, Wind Tunnel and CFD Investigation of the Performance of "Windcatcher" Ventilation Systems, International Journal of Ventilation. 1 (2002) 53–64. http://www.ijovent.org/doi/abs/10.5555/ijov.2002.1.1.53.

[15] H. Montazeri, F. Montazeri, R. Azizian, S. Mostafavi, Two-sided wind catcher performance evaluation using experimental, numerical and analytical modeling, Renewable Energy. 35 (2010) 1424–1435. doi:10.1016/j.renene.2009.12.003.

[16] B.R. Hughes, S.A.A. Abdul Ghani, A numerical investigation into the effect of windvent dampers on operating conditions, Building and Environment. 44 (2009) 237–248. doi:10.1016/j.buildenv.2008.02.012.

[17] J.K. Calautit, B.R. Hughes, Measurement and prediction of the indoor airflow in a room ventilated with a commercial wind tower, Energy and Buildings. 84 (2014) 367–377. doi:10.1016/j.enbuild.2014.08.015.

[18] A.A. Elmualim, Dynamic modelling of a wind catcher/tower turret for natural ventilation, Building Services Engineering Research and Technology. 27 (2006) 165–182. doi:10.1191/0143624406bse159oa.

[19] J.K. Calautit, D. O'Connor, B.R. Hughes, Determining the optimum spacing and arrangement for commercial wind towers for ventilation performance, Building and Environment. 82 (2014) 274–27. doi:10.1016/j.buildenv.2014.08.024.

[20] H.N. Chaudhry, J.K. Calautit, B.R. Hughes, Computational analysis of a wind tower assisted passive cooling technology for the built environment, Journal of Building Engineering. 1 (2015) 63–71. doi:10.1016/j.jobe.2015.03.004.

[21] B.R. Hughes, S. a. a. A. Ghani, Investigation of a windvent passive ventilation device against current fresh air supply recommendations, Energy and Buildings. 40 (2008) 1651–1659. doi:10.1016/j.enbuild.2008.02.024.

[22] M. Afshin, A. Sohankar, M.D. Manshadi, M.K. Esfeh, An experimental study on the evaluation of natural ventilation performance of a two-sided wind-catcher for various wind angles, Renewable Energy. 85 (2016) 1068–1078. doi:10.1016/j.renene.2015.07.036.

[23] A.A.A. Dehghan, M.K. Esfeh, M.D. Manshadi, Natural ventilation characteristics of one-sided

wind catchers: experimental and analytical evaluation, Energy and Buildings. 61 (2013) 366–377. doi:10.1016/j.enbuild.2013.02.048.

[24] Q. Chen, Ventilation performance prediction for buildings: A method overview and recent applications, Building and Environment. 44 (2009) 848–858. doi:10.1016/j.buildenv.2008.05.025.

[25] Liliana Campos-Arriaga, Wind Energy in the Built Environment: A Design Analysis Using CFD and Wind Tunnel Modelling Approach, University of Nottingham, 2009.

[26] B.R. Hughes, J.K. Calautit, S.A. Ghani, The development of commercial wind towers for natural ventilation: A review, Applied Energy. 92 (2012) 606–627. doi:10.1016/j.apenergy.2011.11.066.

[27] M.R. Islam, R. Saidur, N.A. Rahim, Assessment of wind energy potentiality at Kudat and Labuan, Malaysia using Weibull distribution function, Energy. 36 (2011) 985–992. doi:10.1016/j.energy.2010.12.011.

[28] W. ZHIHONG, THE CONTROL OF AIRFLOW AND ACOUSTIC ENERGY FOR VENTILATION SYSTEM IN SUSTAINABLE BUILDING, The Hong Kong Polytechnic University, 2014.

[29] B.M. Jones, R. Kirby, The Performance of Natural Ventilation Windcatchers in Schools - A Comparison between Prediction and Measurement, The International Journal of Ventilation, 9 (2010).

[30] N. Khatami, The Wind-Catcher, A Traditional Solution For A Modern Problem, University of Glamorgan/ Prifysgol Morgannwg, 2009.

[31] J.K. Calautit, B.R. Hughes, H.N. Chaudhry, S.A. Ghani, CFD analysis of a heat transfer device integrated wind tower system for hot and dry climate, Applied Energy. 112 (2013) 576–591. doi:10.1016/j.apenergy.2013.01.021.

[32] K. Sopian, M.Y.H. Othman, A. Wirsat, The wind energy potential of Malaysia, Renewable Energy. 6 (1995) 1005–1016. doi:10.1016/0960-1481(95)00004-8.

[33] T.L. Tiang, D. Ishak, Technical review of wind energy potential as small-scale power generation sources in Penang Island Malaysia, Renewable and Sustainable Energy Reviews. 16 (2012) 3034–3042. doi:10.1016/j.rser.2012.02.032.

[34] J. Franke, A. Hellsten, H. Schlünzen, B. Carissimo, COST Action 732, Best Practice Guideline for the CFD Simulation of Flows in The Urban Environment, Brussels, 2007.

[35] A. Bulińska, Z. Popiołek, Z. Buliński, Experimentally validated CFD analysis on sampling region determination of average indoor carbon dioxide concentration in occupied space, Building and Environment. 72 (2014) 319–331. doi:10.1016/j.buildenv.2013.11.001.

[36] ANSYS Incorporated, ANSYS 14.5 FLUENT Theory Guide, (2015). http://www.ansys.com.

[37] Y. Tominaga, A. Mochida, R. Yoshie, H. Kataoka, T. Nozu, M. Yoshikawa, et al., AIJ guidelines for practical applications of CFD to pedestrian wind environment around buildings, Journal of Wind Engineering and Industrial Aerodynamics. 96 (2008) 1749–1761. doi:10.1016/j.jweia.2008.02.058.

[38] Y. Tominaga, S. Akabayashi, T. Kitahara, Y. Arinami, Air flow around isolated gable-roof buildings with different roof pitches: Wind tunnel experiments and CFD simulations, Building and Environment. 84 (2015) 204–213. doi:10.1016/j.buildenv.2014.11.012.

[39] B.E. Launder, D.B. Spalding, The numerical computation of turbulent flows, Computer Methods

in Applied Mechanics and Engineering. 3 (1974) 269–289. doi:10.1016/0045-7825(74)90029-2.

[40] T. Cebeci, P. Bradshaw, Momentum transfer in boundary layers, Hemisphere Publishing Corp, New York, 1977.

[41] B. Blocken, T. Stathopoulos, J. Carmeliet, CFD simulation of the atmospheric boundary layer: wall function problems, Atmospheric Environment. 41 (2007) 238–252. doi:10.1016/j.atmosenv.2006.08.019.

[42] ASHRAE, ASHRAE standard 62.2, Ventilation and Acceptable Indoor Air Quality in Low-Rise Residential Buildings, in: American Society of Heating, Refrigerating and Air Conditioning Engineers, Atlanta, GA., 2003.

[43] ASHRAE, ANSI/ASHRAE Standard 55-2004 Thermal Environmental Conditions for Human Occupancy, merican Society of Heating, Refrigerating and Air-Conditioning Engineers, 2004.